International Journal of Archaeology
2023; 11(1): 1-8
http://www.sciencepublishinggroup.com/j/ija
doi: 10.11648/j.ija.20231101.11
ISSN: 2330-7587 (Print); ISSN: 2330-7595 (Online)

Analysis of Photoelectric Colorimetry and Fluorimetry of the Turin Shroud

Larry Schwalbe[1, *], Samuel Pellicori[2]

[1]Shroud of Turin Center, Richmond, USA

[2]Pellicori Optical Consulting, Santa Barbara, USA

Email address:

lschwalbe@tampabay.rr.com (Larry Schwalbe), pellopt@cox.net (Samuel Pellicori)

[*]Corresponding author

To cite this article:

Larry Schwalbe, Samuel Pellicori. Analysis of Photoelectric Colorimetry and Fluorimetry of the Turin Shroud. *International Journal of Archaeology*. Vol. 11, No. 1, 2023, pp. 1-8. doi: 10.11648/j.ija.20231101.11

Received: December 28, 2022; **Accepted**: January 13, 2023; **Published**: January 30, 2023

Abstract: We analyze spectrophotometric data collected directly on the Turin Shroud in 1978. Using standard methodologies, we transform 19 visual reflectance and 16 UV-fluorescent emission spectra to CIE xyY color space coordinates. We then compare these results to those of an Italian team of investigators. Comparing x-y chromaticities, the reflectivities from clear areas (background), image, and blood-stain locations agree with corresponding data collected independently by the Italian team. In both sets of data, the clusters from image and background areas overlap strongly and are clearly separated from the blood-stain points. Data from lightly scorched areas fall within the clusters from background and image locations. Data from deeper scorches diverge significantly, as do all scorch data from the Italian team. We generate similar colorimetric data from the spectral UV-fluorescence measurements made by the Shroud of Turin Research Project (STURP). Plotted as x-y chromaticities, the clear areas group together as a cluster as do the blood data but the two clusters show a significant separation from each other. The scorch data are configured along a linear continuum advancing from the lightest clear areas to the darkest scorches. The image data bifurcate: two of the four points lie within the clear-area cluster and the two outliers fall in line with the scorch data. We offer interpretations and speculations on these findings. Quantification of the 1978 measurements establishes a procedure for future monitoring of the aging state of TS features. The measurement protocol and methodologies discussed are important for preservation of other historical art and historical relics.

Keywords: Photoelectric Colorimetry, UV Fluorescence, Turin Shroud, Relic Conservation

1. Introduction

The Turin Shroud (TS) is a long strip of ancient linen containing on one surface the faint, head-to-head, ventral and dorsal images of a man bearing all the marks of torture and death described in the New Testament's account of the passion of Jesus of Nazareth. The Shroud has been revered for centuries by many as the burial cloth of Jesus, but only in recent years has it come under serious scientific scrutiny. A comprehensive report of the 1978 scientific investigation discussing its objectives and results has been published [1]. One objective centers on how the image was produced on the surface of the cloth -- despite many efforts, the question has yet to be answered satisfactorily. The other question, and the focus of the present study, is primarily in the interest of conservation: how best to characterize and document the physical and chemical state of the cloth and its various markings and images. A potential result of the analysis is to assist in narrowing the field of image forming mechanisms by eliminating those that do not exhibit the measured colorimetry and fluorimetry behaviors. We approach these issues by quantifying the color properties of various markings on the TS as determined by specific spectral reflectance and fluorescence measurements.

Colorimetry based on the CIE color space coordinates [2, 3] separates color components that correspond to integrated visual responses. Colorimetry quantifies the visual impressions of hues and their differences, thus facilitating objective comparison among features. Spectrophotometry resolves the measured spectrum into narrow spectral bandwidths (SBW) thereby producing higher analytical

resolution that enables better discrimination between features. Spectrophotometry is useful in providing information potentially applicable in distinguishing chemical and physical causes for color. As applied to archeological objects such as the TS, researchers are interested not only in the origins but also in the conservation of transient features such as cloth color, body image, scorches, water stains, scorched areas, and blood stains. Diagnostic comparisons with the spectral and spatial properties exhibited by paints, pigments, dyes, and adventitious matter and chemistry are made possible.

Optical techniques are applied routinely in many studies of art-historical and conservation interest (see e.g., Freebody [4]). For the Shroud, spectrophotometry and photography have also proven useful in documenting and characterizing the physical and chemical properties of the cloth and its various stains and images [5-13]. Color photography reveals faint visual imagery possessing low-color contrast among features. The present work quantifies these subtle differences focusing primarily on the results of Gilbert and Gilbert [5], the reduction to colorimetric parameters, and comparing those measurements with the published colorimetry of Soardo *et al.* [7].

2. Optical Reflectance Analysis

In 1978, two teams of scientific investigators, one American the other Italian, included in their testing protocols direct photoelectric reflectance measurements on the TS in visual wavelengths. Gilbert and Gilbert [5], who participated as members of the American Shroud of Turin Research Project (STURP), assembled a scanning photoelectric spectrophotometer system. Pellicori (a member of STURP) and Chandos [6, 8] constructed a portable instrument of their own design. The Gilbert reflectometer imaged a 6 x 3 mm area, with 5 nm SBW. Source and image monochromators scanned in tandem to reduce stray light. Illumination was with a 150 W Xenon arc lamp (5500 K). Pellicori and Chandos' imaged area was 1 cm dia. at 17 nm SBW and 20 nm wavelength steps over 420-700 nm. 45^0 illumination was from a 2850 K lamp. Soardo *et al.* [7] probed a 13-mm-dia area with 2850 K illumination.

Pellicori [8] found his results agreeing satisfactorily with those of the Gilberts, but to our knowledge, there has been no attempt yet to compare the results of Gilbert and Gilbert [5] with those of Soardo *et al.* [7]. The likely reason is that the American data are presented as plots of reflectance as functions of wavelength R(λ) whereas the Italians published theirs in integrated form as chromaticity values.

2.1. Analytical Method

To place the data of the Gilberts on parity with those of the Italian investigators, we begin by recognizing that Soardo *et al.* reduced their data from measurements referenced to a diffuse white standard. The Gilberts present spectra for background areas as "absolute reflectances," that is, relative to an MgO "white" standard. Data for non-background features are presented as "relative spectral reflectances" with the background contributions removed, that is, relative to the cloth background values. Because the Gilberts' [5] original spectra are unavailable for processing, we approximate them by incorporating the mean reflectivity of five background areas plotted in their figure 6. (We comment on the uncertainties using this approach below.) For each of the Gilberts' spectra R(λ), we digitize the graphic at each node point and then interpolate at 5-nm intervals between 380 and 780 nm. In these numerical forms, we simulate the original data by multiplying the relative and average background values at each wavelength.

The next step for each reconstructed spectrum is to evaluate the corresponding three-color coordinates, or tristimulus values, in the CIE XYZ color space:

$$X_E = \frac{1}{N} \cdot \sum_{\lambda=380\ nm}^{780\ nm} \bar{x}(\lambda) \cdot R(\lambda)\, \Delta\lambda$$

$$Y_E = \frac{1}{N} \cdot \sum_{\lambda=380\ nm}^{780\ nm} \bar{y}(\lambda) \cdot R(\lambda)\, \Delta\lambda \qquad (1)$$

$$Z_E = \frac{1}{N} \cdot \sum_{\lambda=380\ nm}^{780\ nm} \bar{z}(\lambda) \cdot R(\lambda)\, \Delta\lambda$$

$$\text{where } N = \sum_{\lambda=380\ nm}^{780\ nm} \bar{y}(\lambda)\, \Delta\lambda$$

In these equations, Δλ = 5 nm, and $\bar{x}(\lambda)$, $\bar{y}(\lambda)$, and $\bar{z}(\lambda)$ are the color-matching functions as defined by the CIE in 1931 for the "standard observer" [2, 3]. Listings of the color-matching functions are readily available online; we downloaded those found in Walker [14].

In general, the treatment also incorporates a wavelength-dependent illumination factor. Our calculation, thus far, assumes a uniform spectral illumination, corresponding the CIE standard illuminant "E," which we indicate by the subscript. Soardo *et al.* [7] refer their data to the non-uniform illuminant "A", which corresponds to the black-body spectrum at T = 2856 K. We convert our calculated (X_E, Y_E, Z_E) to (X_A, Y_A, Z_A) using the Bradford transformation matrix listed by Lindbloom [15].

The final step is to compute chromaticities (x, y, z), which is essentially a normalization operation:

$$x = \frac{X_A}{X_A+Y_A+Z_A}$$

$$y = \frac{Y_A}{X_A+Y_A+Z_A} \qquad (2)$$

$$z = \frac{Z_A}{X_A+Y_A+Z_A}$$

Since z = 1 – x – y, we observe that the three originally independent parameters have been reduced to two in this color-space representation. To preserve all the information available, we proceed in the more complete xyY color space.

2.2. Results and Discussion

Table 1 contains all the results we derive from the reflectance data in the Gilberts' 1980 report [5]. The first column in the table identifies the number of the figure in their paper where each spectrum appears; column 2, the code

designator for each test point located in their Figure 18; column 3, the type of stain at that location; columns 4-6 the coordinates in the xyY color space. The x- and y-components fall in the red section of the CIE chromaticity diagram. The Y component indicates luminosity.

Table 1. *Results of transforming the spectral reflectivity data of Gilbert and Gilbert [5] to xyY color space coordinates.*

G-G Fig.	Location	Type	x	y	Y
6	Mean	Clear	0.4794	0.4174	0.3789
6	F4	Clear	0.4767	0.4170	0.4099
6	B1F	Clear	0.4808	0.4169	0.3729
8	Mean	Image	0.4871	0.4180	0.3264
8	Mean	Scorch	0.4876	0.4177	0.3193
10	B1E	Image	0.4851	0.4176	0.3401
10	F3A	Image	0.4831	0.4183	0.3071
10	F8F	Image	0.4910	0.4189	0.3162
10	B1D	Image	0.4901	0.4178	0.2643
12	B3E1	Scorch	0.4853	0.4174	0.3379
12	B3E	Scorch	0.4873	0.4179	0.3239
12	F8H	Scorch	0.4908	0.4176	0.3000
12	B1C	Scorch	0.4973	0.4166	0.2765
12	F3D	Scorch	0.5130	0.4162	0.1773
14	Mean	Blood	0.5038	0.4106	0.2570
16	B1A	Blood	0.4997	0.4137	0.3160
16	F8C	Blood	0.5029	0.4112	0.2669
16	F3E	Blood	0.5061	0.4095	0.2570
16	F6B	Blood	0.5078	0.4095	0.2339

The plot in Figure 1a compares the present chromaticity results (solid symbols) with selected data from Soardo *et al.* [7] (open symbols). We have not included uncertainty limits with these data, largely because of the limited information available in the publications. However, we can provide estimates from the step we took using the mean background spectrum to "reconstruct" the Gilberts' raw data. In their figure 6, the Gilberts show an approximate offset of 0.02 between the spectrum from location F4 and that of the mean clear area. If we use that number as an estimate of the offsets of the actual backgrounds from the mean backgrounds in our reconstructed data, we introduce an uncertainty of roughly ± 0.0005 in the x-chromaticity component and ± 0.0015 in the y.

We observe generally good agreement between the distributions for the background, image, and blood data from the two measurement sets, well within the limits of the uncertainties. As Soardo *et al.* [7] illustrated earlier, the cluster of blood data shows a clear separation from the strongly overlapping background and image clusters. The overlapping effect of the latter (Figure 1b) is consistent with the conclusions of the 1978 investigations [1, 16] that the image and background areas are similar in their chemical nature. The relatively large scatter in the Soardo data may result from the mottling of the background color (as is evident in the UV fluorescence photo below).

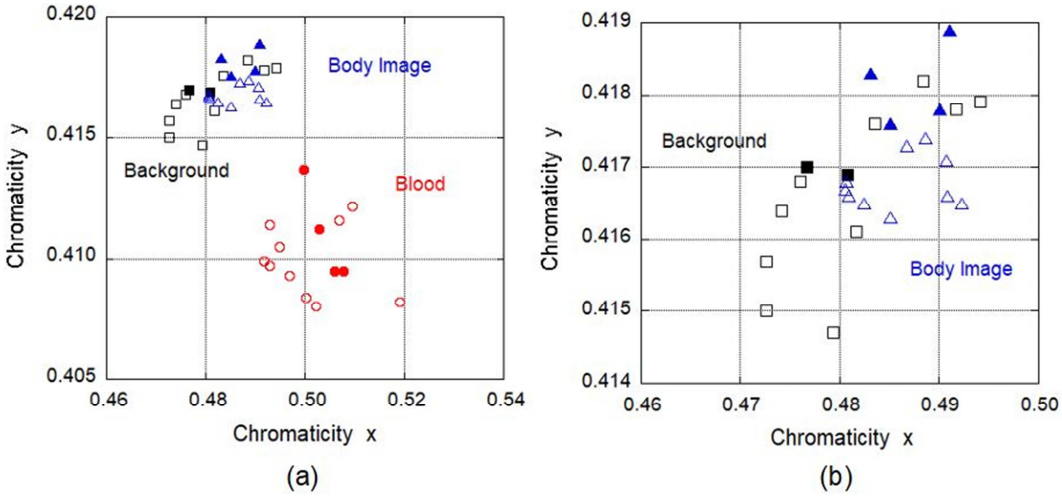

Figure 1. *(a) Plots of chromaticities derived from Gilbert and Gilbert [5] (solid symbols) and selected values from Soardo et al. [7] (open symbols) for background (black squares), body image (blue triangles), and blood (red circles). (b) Expanded scales for body and background cloth values.*

The Y color coordinate, presented in the final column of Table 1, measures the "lightness" or the magnitude of the reflectivity of a test location. Although the data are admittedly sparse, the background locations F4 and B1F have values Y = 0.4990 and 0.3729, respectively, compared with an average value of Y = 0.31 ± 0.03 for image areas. Their difference ΔY indicates a small, but significant (and visible) contrast between background and image. The value of the differential ΔY and its changes are crucial because age and environmental exposure continuously degrade (dehydrate and oxidize) the cellulose of the linen cloth causing the ΔY between image and background to decrease. A decrease indicates the image is becoming less visible in contrast to the background. Therefore, as differences in the Y-parameter values provide a measure of the image contrast, we suggest that ΔY be regarded as a potential diagnostic in the conservation monitoring practices.

Figure 2a compares chromaticities derived from the body-image and scorch data of Gilbert and Gilbert [5]. As expected from the plot in the Gilberts' figure 8, the close correspondence of their mean image and light-scorch data is reflected by the proximity of the present results (indicated by the closed symbols). Trending to higher x- and lower y-chromaticities, indicating redder hues, we observe two outliers derived from the more heavily scorched locations at B1C and F3D.

Figure 2b shows an expanded view to include four scorch (or burn) data from Soardo *et al.* [7], their locations P 007, P 010, P 032, and P 040. Although neither the locations nor the intensity of scorching for these points are specified in their report, the large separation from image and light-scorch clusters -- and the closer correspondence to the more heavily scorched Gilbert data -- suggests that pyrolysis tended toward burning temperatures as indeed these areas are blackened. That pyrolysis presumably occurred under the limited oxygen conditions that likely were present during the fire of 1532 that scorched the folded TS while contained in the silver box [1, 16]. Artificial aging of linen in the lab produces progressively greater reddening with increasing temperature and time [8].

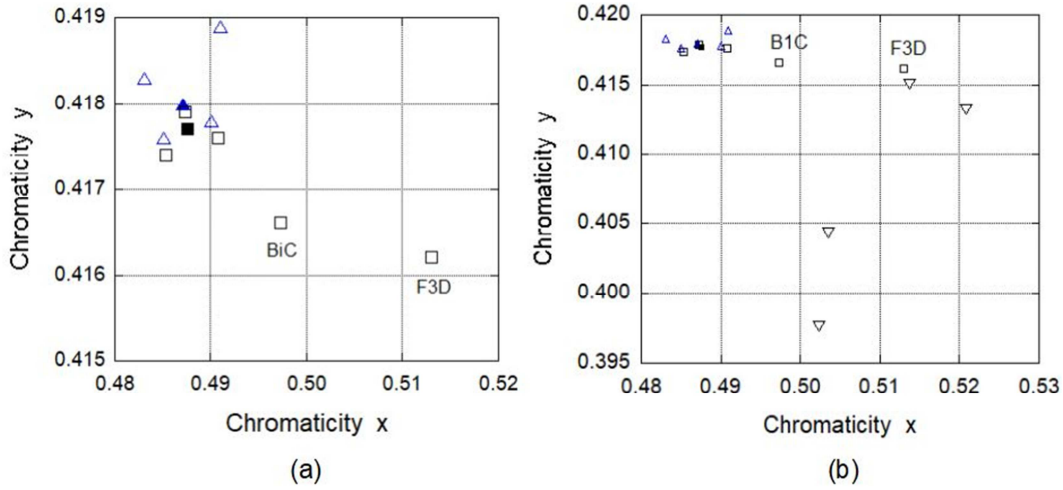

Figure 2. *(a) Plot of chromaticities derived from Gilbert and Gilbert [5] at image (open upward-pointing triangles) and scorch locations (open squares). Solid symbols represent average values. (b) Expanded plot includes data from Soardo et al. [7] shown as downward pointing triangles.*

3. UV-Stimulated Visual Fluorescence

Ultraviolet-stimulated fluorescent (UVF) emission is capable of distinguishing differences in chemical compositions through emission and absorption spectra. As a sensitive diagnostic tool in many applications, the method is likewise important in the broad effort to characterize and distinguish the physical and chemical states of the TS fabric and its various stains. Conservators especially should understand the chemical makeup of the fluorescing elements and whether they derived from the raw materials in the cloth's manufacture, the manufacturing process itself or from subsequent environmental conditions such as microbial contamination. Similarly, any changes in the fluorescent properties should be monitored to alert against the onset or the advance of potentially damaging agents or storage / display conditions.

3.1. Visual and Photographic Studies

To date, the only direct measurements of UVF from the TS are those acquired in 1978 by the STURP team [5, 11]. Miller and Pellicori [11] published color reproductions of seven UVF photographs from various locations and paired these with visible-light photos from the same areas. Figure 3 (left) shows the UVF image containing face, chest, patches, burned areas, and a water stain on the background cloth. As is evident in the figure, the UVF images reveal contrasting details beyond those in the visible light reflectance photos as well as color differences of fluorescing materials.

In addition to photographs, Miller and Pellicori documented their direct-visual observations. To compare these observations with those we derive from the spectrophotometry, we limit our focus to their comments regarding the four general features where the two studies overlap:

While recording their photographs, Miller and Pellicori noted that the clear-areas (non-image or background) appear a yellow-green hue. As discussed below, the published UVF photos show background colors tending more strongly to bluish hues.

Body-image areas appear to have no fluorescing color unlike the sepia or straw-like tint observed in the reflected visible light photos [13]. The image areas are absorbing and not themselves fluorescing. The UVF photos present greater contrast between the image and adjacent background than do those taken with visible-light (see Figure 3).

Scorches appear dark brown visually and the faintly scorched areas fluoresce brownish-red. Open burn holes of regions 6 and 16 exhibit total absorption. The color reddens as the scorch density decreases. The density- and color-grading effect may be attributed to the transition of cellulose pyrolytic decomposition products, such as furfurals, and other compounds produced under limited oxygen conditions between low and combustion temperatures.

Blood stains are highly absorbing and show no UVF color. Fluorescing borders are apparent around some areas that might be plasma flows [1].

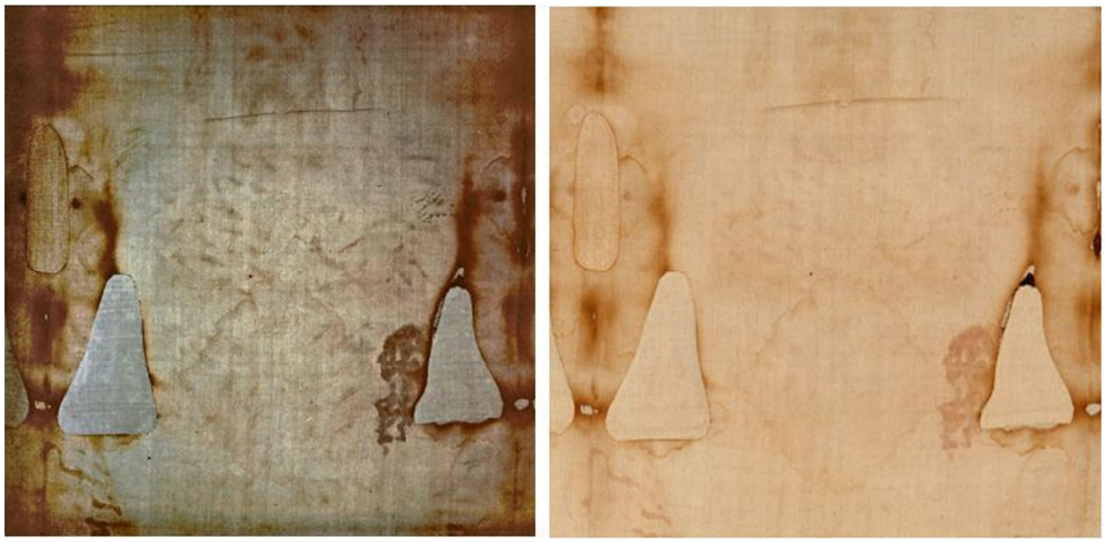

Figure 3. *UVF emission and visible-light reflectance photographs in the ventral, chest region. Striping in the weave evident in the UVF image complicates the "background – clear" cloth measurements. Patches covering burned areas are repairs made in 1534.*

3.2. Spectrometric Fluorescence

Along with photoelectric reflectance, Gilbert and Gilbert [5] included UVF measurements at selected locations: four in clear areas (their figure 7), four in image areas (figure 11), five in scorched areas (figure 13), and three in blood-stained areas (figure 17). As with the reflectance data, each test point is assigned a code identifier and its location on the TS surface is documented in their figure 18.

For all spectra, the excitation wavelength was 365 nm, and data were collected through the wavelength range 400-700 nm using a dual monochromator to isolate the emission and excitation energies and stray light. The results were reported in arbitrary units referenced to the clear-area measurement at the location designated as F4. Referring to figure 18 in the Gilbert-Gilbert report, F4 is located roughly half-way distant between the right forearm of the ventral image and the long edge of the cloth.

To reduce the fluorescence spectra to equivalent chromaticity values and visual intensities, we digitize Gilbert's graphically depicted data. We use an analytical method slightly modified from that described for the reflectivities in section 2.1. Specifically, in Eq. (1), we replace the reflectivity function $R(\lambda)$ with the intensity of the emitted fluorescent light $E(\lambda)$, and we exclude any transformation to an illumination standard. The results of the analyses are presented in Table 2. Note that we denote the color space as xyY*, where the asterisk indicates the quantity Y relative to the arbitrary units that the Gilberts used in their report. The x- and y-coordinates correspond to bluish-green on the CIE chromaticity diagram.

An early objective of our study was to use the UVF photographs of Miller and Pellicori [11] to convert the units of the visual-intensity parameter Y* from arbitrary to physically meaningful quantities. However, variables in color rendition introduced by the processing and subsequent reproduction of the photos rendered this approach uncertain. We therefore continue our discussion using the relative scale for Y* shown in Table 2 and confine our data comparisons to the comments that Miller and Pellicori include in their report.

Table 2. *Results of transforming the fluorescence data of Gilbert and Gilbert [5] to xyY* color space coordinates.*

G-G Fig.	Location	Type	x	y	Y*
7	F4	Clear	0.2390	0.2675	0.1831
7	F3B	Clear	0.2393	0.2763	0.1727
7	F6D	Clear	0.2424	0.2741	0.1496
7	B1F	Clear	0.2362	0.2687	0.1325
11	B1E	Image	0.2424	0.2769	0.1556
11	B6A	Image	0.2493	0.2902	0.1465
11	F8F	Image	0.2563	0.2957	0.1244
11	B1D	Image	0.2386	0.2712	0.0882
13	B3E	Scorch	0.2593	0.3000	0.1650
13	F8H	Scorch	0.2615	0.2982	0.1327
13	F3C	Scorch	0.2697	0.3072	0.1055
13	B1C	Scorch	0.2840	0.3236	0.0830
13	F3D	Scorch	0.3126	0.3472	0.0558
17	F8C	Blood	0.2529	0.2787	0.1021
17	F3E	Blood	0.2528	0.2809	0.0828
17	F6B	Blood	0.2545	0.2795	0.0727

As stated above, the UVF photographs that Miller and Pellicori published display a blue-green color in the background areas. The original UVF photography used color negatives with a 2¼-in format size. From these negatives, Miller made 4 x 5-in color positives and 35 mm slides of the same areas. Pellicori digitized the 35-mm slide photos for subsequent analysis. His objective was to adjust the visual background hue of the UVF images to correspond to the visually observed hue [11]. To simulate the photographic result, Pellicori began with the fluorescent emission spectrum at the clear F4 location (Figure 4a). He then modeled the photographic spectral response of the UV-absorbing, visible-transmitting filter placed in front of the camera. The purpose of the filter was to eliminate the UV reflection from the illuminated area at wavelengths shorter than about 410 nm. Finally, Pellicori rescaled the transmitted spectrum by the wavelength response of the film.

Figure 4b shows the results of these operations. The UV filter produces the most dramatic effect by suppressing the emission below 410 nm, thereby generating the steep rise in the simulated spectrum to its maximum near 460 nm. In the range of longer wavelengths, more subtle effects are evident: the film response enhances the green component of the effective emission (ca. 460-550 nm) and suppresses the red component (>590 nm) slightly.

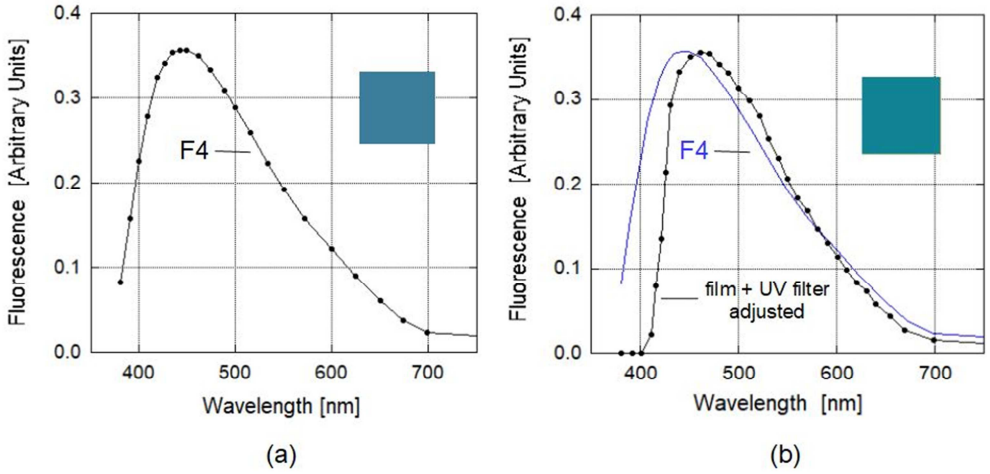

Figure 4. *(a) Fluorescence spectrum at F4, clear background area, with color rendition, and (b) F4 and F4 modified to represent the film-response function.*

Figure 4 allows us to compare the implied color differences. Keeping in mind the arbitrary nature of the brightness coordinate Y*, we only compare the differences in hue between the baseline spectrum at F4 and the modified function in Figure 4b. The differences in color are quite subtle, and we recommend the reader use an online rendering utility such as www.colorizer.org, as we did to generate the color patches. The color coordinates for F4 in Table 2 produce the blue color patch shown in Figure 4a; for the modified spectrum in 4b, we use the xyY* coordinates (0.2362, 0.2927, 0.1927) that we derive from the result in 4b and our spectrum-analysis program. We observe the simulated background color showing a subtle, but discernable, shift from the F4 blue toward the green.

The x-y chromaticity coordinates for all background, image, scorch, and blood locations in Table 2 are plotted in Figure 5. In the limited-scale plot of 5a, we observe a cluster of background points (black open squares) exhibiting a variation that we believe results from the ubiquitous color mottling in most, if not all, of the background areas especially evident in the UVF photos: Figure 3 and Ref. [17].

The blood data show a tighter cluster than do the background data and a clear separation from them toward the red. Miller and Pellicori [11] state that the blood does not fluoresce, an observation we accept. Rather than attributing this shift toward the red to an inherent fluorescence from the blood, we believe that light from the underlying cloth is simply being attenuated by the blood's stronger absorption in the shorter wavelength region [5, 8].

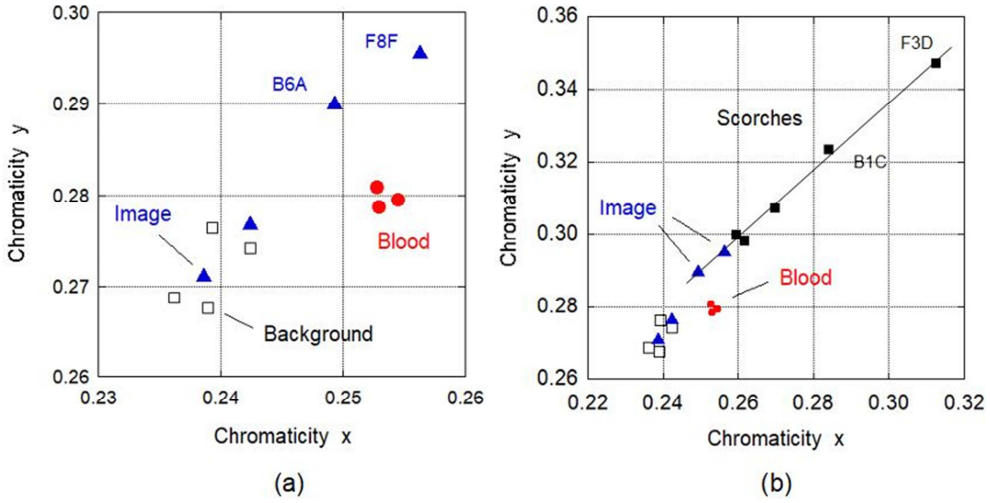

Figure 5. *(a) Plots of chromaticities from Table 2 for background, image, and blood, (b) expanded chromaticity plot including the five scorch-area data.*

Also in Figure 5a, the image data show an interesting bifurcation: two image points with lower x and y values, B1E and B1D, lie within the cluster of background points, whereas the remaining two, B6A and F8F, lie well

separated from the cluster to larger x-y values, indicating redder hues. An interesting aspect of the bifurcation is the mix: each pair consists of one relatively high fluorescent intensity Y*, point (B1E and B6A) and one relatively low (F8F and B1D). Considered together, the reflectance and fluorescence data for the image and background sets are difficult to interpret in a consistent manner. On the one hand, the reflectances of the image and background each show a relatively consistent internal structure, although their centroids are displaced slightly (Figure 1a). On the other hand, the bifurcation of the fluorescent data for the image data (Figure 5b) may suggest a slight inhomogeneity in their chemical compositions.

In Figure 5b, we include the five data from scorched locations. Two observations stand out: first, the x-y coordinates of the scorch data increase in a near linear fashion (and at a 45-deg angle) with increasing scorch depth. Second, a short extrapolation of the scorch data beyond their lower or "light" end includes the two outlying image points where the color difference are very small.

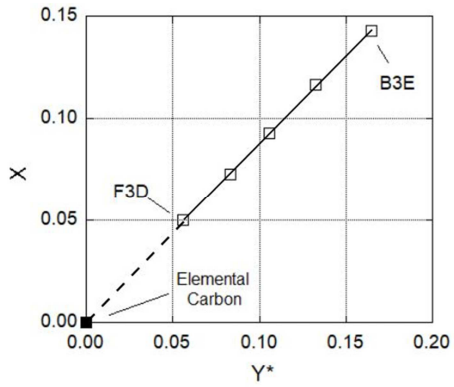

Figure 6. *Plot of the X-Y tristimulus values for five scorch-area data plus the "black" point corresponding to elemental carbon.*

The functional behavior of the scorch data is readily understood. Suppose we consider these data as samples representing different arrested stages of pyrolysis. Recall the parameters X, Y, and Z that we derive using Eq. (1) above. Technically these represent the intensities of the human visual responses to the colors red, green, and blue, respectively. In the xyY color space, however, the Y parameter defines the "lightness" of a color. Suppose we take Y, running in the negative direction, to represent a progress variable that measures the degree to which the textile, and its fluorescing component, have been transformed from an initial pristine state toward an end state of elemental carbon. Retaining X, say, as a measurable property at each stage of combustion, the results plotted in Figure 6 show a near linear behavior that incidentally extrapolates to the origin, which represents zero fluorescent intensity, that is, the black (total absorption) of elemental carbon. We recover the x-y plot of the scorch data in Figure 5b by uniformly scaling the two axes of Figure 6 and rotating the plot about X = Y*.

Miller and Pellicori [11] state that the dark scorches (burns) do not fluoresce and that the more lightly scorched areas -- with a darkness like that of the body image -- fluoresce with a faint reddish hue. This behavior is visually evident in the UVF photos (see e.g., Figure 3). To explain the effect, these investigators suggest it may be attributed to pyrolysis products, such as furfurals, produced within a limited-oxygen environment at high temperature as mentioned above [1, 16]. This hypothesis of reddish fluorescing pyrolysis products is quite acceptable because the shorter wavelengths are more strongly absorbed in these reaction products, thus there is less green and blue emission contributed by the background, while the red emission is nearly constant. This behavior is expected for pyrolytic decomposition and reaction products of cellulose, and evidently reaches a saturation point at the high temperature black borders of scorches where all short-wavelength light is absorbed. The UVF photos confirm that the darkest scorches do not fluoresce any color, they are black. Only the faintest scorches fluoresce a faint reddish hue – this result contrasts with the body image which only absorbs and does not itself fluoresce.

Miller and Pellicori [11] state that their UVF photos show a difference in contrast between the image and the adjacent background areas that looks to be greater than the contrast seen in the visible-light photographs. To illustrate, the visual image in Figure 3 shows relatively little contrast between body and background (clear) areas: the contrast is subtle and the colors are similar. As stated above, that contrast is expected to decrease with age and environmental exposure. For conservation purposes, it is important to monitor the effects of external influences on the visibility of the body image. The body image and other features are revealed with higher contrast in the UVF image of Figure 3, suggesting greater sensitivity for detecting differences and temporal changes. We compare the relative color contrasts within the visible and the UVF images, where contrast C = (Max – Min) / (Max + Min). Using the x component of the color coordinates, the color image-to-background contrast revealed by the UVF measurements is 2.6 times the similar visible image contrast, $C_{UVF} / C_{vis} = 2.6$.

4. Summary and Conclusions

We analyze the spectrophotometric measurements from the 1978 STURP investigation along with simultaneous UVF photography to produce quantitative data useful in efforts to preserve the material integrity of the TS and its image features. We transform the graphical data of Gilbert and Gilbert [5] to a digital format and generate CIE coordinates for each data set in the xyY color space. For the reflectance data, we find good correspondence between the results from STURP with those collected at the same time by an Italian team. Together they confirm the main conclusions that the faint image and background points overlap whereas the blood areas show no hue component overlap; instead, they are displaced significantly away from the image-background sets. Data from lightly scorched areas overlap image data whereas those from the more heavily burned areas are redder and diverge significantly.

The fluorescence data show some similarities with the reflectance. The background points form a relatively close cluster located well away from an extremely tight blood cluster. The image data bifurcate oddly; two of the four data lie within the background cluster, but the remaining two lie a significant distance away and seem to be more aligned with the collection of faint scorch data. The scorch data exhibit a linear behavior directed away from the image and background sets. We present an analysis to explain the effect. The overall results support the hypothesis that the image areas contain a lower concentration of oxidation and conjugation products of cellulose than is produced in the higher temperature scorched areas [1, 6, 8, 16]. The chemical reaction in the image is insufficient to emit a fluorescent signal. The results of the colorimetry and fluorescence analyses support an image formation mechanism different from that which high temperature scorching would produce.

The results of this study rest on photoelectric measurement techniques that are routinely applied to objects of art-historical interest. We anticipate that multi-spectral reflectometry and UVF fluorimetry and photography will continue to be applied and be augmented by even newer technologies as they come online. Together the growing database characterizing the physical and chemical state of the TS will stand as a foundation of information in support of a well-planned and adequately funded program to preserve the TS in its current condition.

Disclosure

The authors declare no conflicts of interest.

Acknowledgements

The authors thank Barrie M. Schwortz documentary photographer also a member of STURP, for allowing us to include his copyrighted white-light photograph in Figure 3 (right) and for making his website www.shroud.com available for downloading all the digitized spectral data we generated from Gilbert and Gilbert [5].

References

[1] Jumper, E. J., Adler A. D., Jackson J. P., Pellicori S. F., Heller J. H., and Drusik J. R., "A Comprehensive Examination of the Various Stains and Images on the Shroud of Turin," *Archaeological Chemistry III, ACS Advances in Chemistry* No. 205, J. B. Lambert, Editor, Chapter 22, American Chemical Society, Washington D. C., 1984, pp. 447-476.

[2] Commission Internationale de l'Éclairage (CIE). Publication No. 15, Colorimetry, 1986, 1971. (CIE 1986).

[3] Commission Internationale de l'Éclairage (CIE). "Standard on Colorimetric Observers," CIE S002, (1986).

[4] Freebody, M., "More than Skin Deep: Photonics Protects our Cultural Heritage," www.photonics.com/issues/photonics_spectra_august_2022/i1 361 (2022).

[5] Gilbert, Jr, R., and Gilbert, M., "Ultraviolet-Visible Reflectance and Fluorescence Spectra of the Shroud of Turin," *Applied Optics* 19, pp. 1930-1936 (1980).

[6] Pellicori, S. F., and Chandos, R. A., "Portable Unit Permits UV/vis Study of the 'Shroud'" reprinted from *Industrial Research & Development* – February 1981.

[7] Soardo P., Iacomussi P., and Rossi G., "Colourimetry of the Shroud" in "The Shroud, past, present and future," International Scientific Symposium, Torino, 2-5 March 2000 – Effatá Editrice, Cantalupa (TO) pp. 89-100 (2000).

[8] Pellicori, S. F., "Spectral Properties of the Shroud," *Applied Optics 19* (12), pp. 1913-1920 (1980).

[9] Privitera, C., "Digital Colorimetric Analysis of the Shroud of Turin," *MATEC Web of Conferences 36,* DOI 1051/matecconf/20153602002 (2015).

[10] Devan, D. and Miller, V., "Quantitative Photography of the Shroud of Turin," *IEEE 1982 Proceedings of the International Conference on Cybernetics and Society*, pp. 548-553, (October 1982).

[11] Miller, V. D. and Pellicori, S. F., "Ultraviolet Fluorescence Photography of the Shroud of Turin," *Journal of Biological Photography 49* (3), pp. 71-85, (1981).

[12] Pellicori, S., and Evans M. S., "The Shroud of Turin Through the Microscope," *Archaeology,* pp. 34-43, (January/February 1981).

[13] ©1978 Barrie M. Schwortz Collection, STERA, Inc.

[14] Walker, J., "Color Rendering of Spectra," https://www.fourmilab.ch/documents /specrend/ (1996).

[15] Lindbloom, Bruce J., "Chromatic Adaptation," www.brucelindbloom.com (revised 2017).

[16] Schwalbe, L. A., and Rogers, R. N., "Physics and Chemistry of the Shroud of Turin," *Analytica Chimica Acta 135*, pp. 3-49, (1982).

[17] Samuel Pellicori, "UV Fluorescence Imagery of the Turin Shroud – Digitally Revisited" International Journal of Archeology, Vol 8, No. 2, 32-36 (2020) doi 10.11648/j.ija 20200802.13.